Physical and Thermal Properties of L-Lactide/ε-Caprolactone Copolymers: The Role of Microstructural Design

Sawarot Phetsuk[a], *Robert Molloy*[a,b], *Kanarat Nalampang*[a,b], *Puttinan Meepowpan*[a,b], *Paul D. Topham*[c], *Brian J. Tighe*[d] *and Winita Punyodom*[a,b]*

[a)] *Department of Chemistry, Faculty of Science, Chiang Mai University, 50200, Thailand*

[b)] *Center of Excellence in Materials Science and Technology, Chiang Mai University, 50200, Thailand*

[c)] *Aston Institute of Materials Research, Aston University, Birmingham, B4 7ET, UK*

[d)] *Chemical Engineering & Applied Chemistry, Aston University, Birmingham, B4 7ET, UK*

Corresponding author e-mail: winitacmu@gmail.com

Keywords: Ring-opening polymerization, L-lactide/ε-caprolactone copolymers, tin(II) *n*-butoxide, microstructural design

Abstract

Understanding the underlying role of microstructural design in polymers allows for the manipulation and control of properties for a wide range of specific applications. As such, this work focuses on the study of microstructure-property relationships in L-lactide/ε-caprolactone (LL/CL) copolymers. One-step and two-step bulk ring-opening polymerization (ROP) procedures were employed to synthesize LL/CL copolymers of various compositions and chain microstructures. In the one-step procedure, LL and CL were simultaneously copolymerized to yield P(LL-*stat*-CL)

statistical copolymers. In the two-step procedure, poly(L-lactide) (PLL) and poly(ε-caprolactone) (PCL) prepolymers were synthesized in the first step before ε-CL and LL respectively were added in the second step to yield P[LL-*b*-(CL-*stat*-LL)-*b*-LL] and P[CL-*b*-(LL-*stat*-CL)-*b*-CL] block copolymers as the final products. The findings reveal that in addition to the copolymerization procedure employed, the length and type of the prepolymer play important roles in determining the chain microstructure and thereby the overall properties of the final copolymer. Moreover, control over the degree of crystallinity and the type of crystalline domains, which is controlled during the polymer chemistry process, heavily influences the physical and mechanical properties of the final polymer. In summary, this work describes an interesting approach to the microstructural design of biodegradable copolymers of LL and CL for potential use in biomedical applications.

1. Introduction

Nowadays, synthetic biodegradable polyesters are widely used in a myriad of biomedical applications.[1-3] Poly(L-lactide) (PLL), poly(ε-caprolactone) (PCL) and polyglycolide (PG) are all important aliphatic polyesters that can degrade in the human body.[4-6] In any biomedical application, it is necessary to verify that the initial mechanical properties of the biodegradable device are sufficient to meet the needs of the application and can be retained for as long as required.[7-8] Molecular weight (and its distribution) is one of the most important properties that defines the strength of a polymeric material. Generally, ring-opening polymerization (ROP) of cyclic esters with a variety of catalysts and initiators is employed to produce high molecular weight polyesters.[9-10] One such initiator, as used in this work, is tin(II) *n*-butoxide [Sn(O*n*Bu)$_2$] which can be employed to produce polymers with controlled molecular weight ($\bar{M}_n$) in the range of 10^3 to 10^6 Da.[11]

In addition to molecular weight, the microstructural design of biodegradable polymers is another key element for biomedical applications.[7-8,12] It is well-known that PLL is a brittle polymer of high modulus and low percentage elongation, while PCL is slow to biodegrade and is a flexible, low melting point polymer, properties which limit their respective applications as homopolymers.[13] To broaden their range of applications, copolymerization of L-lactide (LL) and *ε*-caprolactone (CL) to produce poly(L-lactide-*co*-*ε*-caprolactone), P(LL-*co*-CL), is an effective way of producing materials with the desired properties by tailoring their microstructures.[13-16] Lin *et al*.[17] demonstrated the effects of copolymer composition and chain microstructure on the crystallization behavior as well as the thermal and mechanical properties of P(LL-*co*-CL) of various compositions. Fernández *et al*.[18] reported that mechanical properties and degradability could be improved by increasing the CL content, while the use of a higher polymerization temperature resulted in a more random monomer sequencing in P(LL-*co*-CL).[19]

In other previous studies, a P(CL-*b*-LL) block copolymer was prepared via a two-step polymerization in which PCL was generated as a prepolymer in the first step. Reversal of the monomer addition using a PLL prepolymer as the propagating species gave a more random structure which was attributed increased to transesterification during copolymerization.[20-26] Other researchers have also attempted to synthesize P(LL-*b*-CL) using PLL as a propagating species, employing either rare earth metal-based initiators or specially designed, sterically hindered tin(IV) initiators.[27-29] Florczak *et al*.[30] also demonstrated the possibility of synthesizing a P(LL-*b*-CL) block copolymer where the LL monomer was polymerized first using an initiating system of aluminum tris-isopropoxide [$Al(O^iPr)_3$] and (*S*)-(+)-2,2′-[1,1′-binaphtyl-2,2′diylbis(nitrylomethilidyne)]diphenolate [$SB(OH)_2$] which exhibited increased selectivity due to the bulky $SB(OH)_2$. In another approach, a the coupling reaction between PCL, PLL and *α*,*ω*-

ditelechelic oligomers was proposed as a possible route to PLL-PCL multiblock copolymers which exhibited beneficial properties for use as thermoplastic elastomers, porous materials, and drug delivery systems.[31-32]

In this present study, LL/CL copolymers of various compositions have been synthesized via the bulk ROP of LL and CL using $Sn(O\textit{n}Bu)_2$ as the initiator. Both one-step and two-step procedures were employed to synthesize LL/CL copolymers with different chain microstructures. The sequence of monomer addition was also varied in order to compare the effect of the type of prepolymer on the final copolymer microstructure. However, it is in how this sequential monomer addition is managed that the novel aspect of this work lies. As an enhancement to the conventional procedure in which the first monomer is totally consumed before the second monomer is added, this paper now describes how, by controlling the % conversion of the first monomer, a whole range of block copolymers with different microstructures and subtly different properties can be obtained. This level of versatility in microstructural design is especially important in biomedical applications where the polymer needs to be tailor-made to meet specific property requirements.

2. Experimental

2.1. Materials

LL was synthesized from L-lactic acid (Carlo Erba, optical purity 97%) and recrystallized from ethyl acetate three times before being dried in a vacuum oven until at least 99.9% chemical purity was obtained, as verified by differential scanning calorimetry (DSC). CL (Acros) monomer was distilled under reduced pressure and stored under a dry nitrogen atmosphere at room temperature. The $Sn(O\textit{n}Bu)_2$ initiator was synthesized according to the method described in the work of Gsell *et al*.[33]

2.2 Synthesis of LL/CL copolymers

PLL and PCL homopolymers and LL/CL copolymers were synthesized via bulk ROP of LL and CL using 0.10 mol % of tin(II) *n*-butoxide [Sn(O*n*Bu)$_2$] as the initiator. For statistical copolymerization, the LL:CL comonomer feed molar ratio was varied as 1:2, 1:1, 1.5:1 and 2:1. Polymerizations were carried out in 25 ml round-bottomed flasks with magnetic stirring under a dry nitrogen atmosphere. The total amount of monomer (LL and/or CL) in each reaction was 20 g. In this work, two different procedures were employed. In the one-step procedure, LL and CL were mixed together with Sn(O*n*Bu)$_2$ at the beginning of the polymerization and the reaction flasks immersed in an oil bath at 120 °C for 12 h. The reaction for this one-step procedure is shown in Scheme 1.

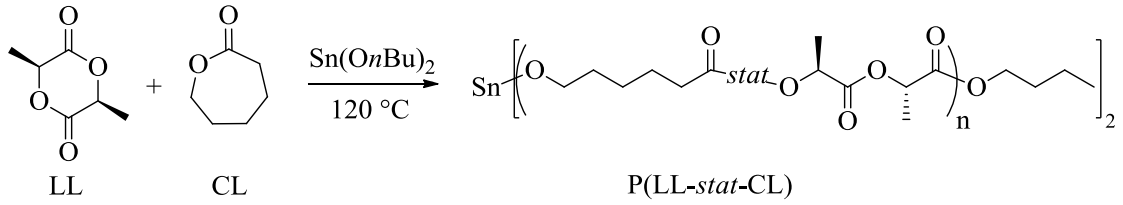

Scheme 1. One-step copolymerization for P(LL-*stat*-CL) statistical copolymer

In the two-step procedure, the first monomer was polymerized to approximately 25 or 70 % conversion, as verified by ^{1}H-NMR, before the second monomer was added and the reaction continued for a total of 12 h. The polymerization time for the first monomer varied from 5-50 minutes depending on which monomer (LL or CL) was polymerized first since the monomer reactivities (LL > CL) are markedly different. This two-step procedure in which LL was

polymerized first to give a PLL prepolymer before the CL was added in the second step is shown in Scheme 2.

In the second step, the CL monomer together with the remaining LL monomer from the first step are inserted into the Sn-O bonds according to the widely-accepted coordination-insertion mechanism.[11,34] After polymerization, the crude products were purified by dissolving in chloroform and re-precipitating in cold methanol before being filtered and dried in a vacuum oven at 45 °C to constant weight.

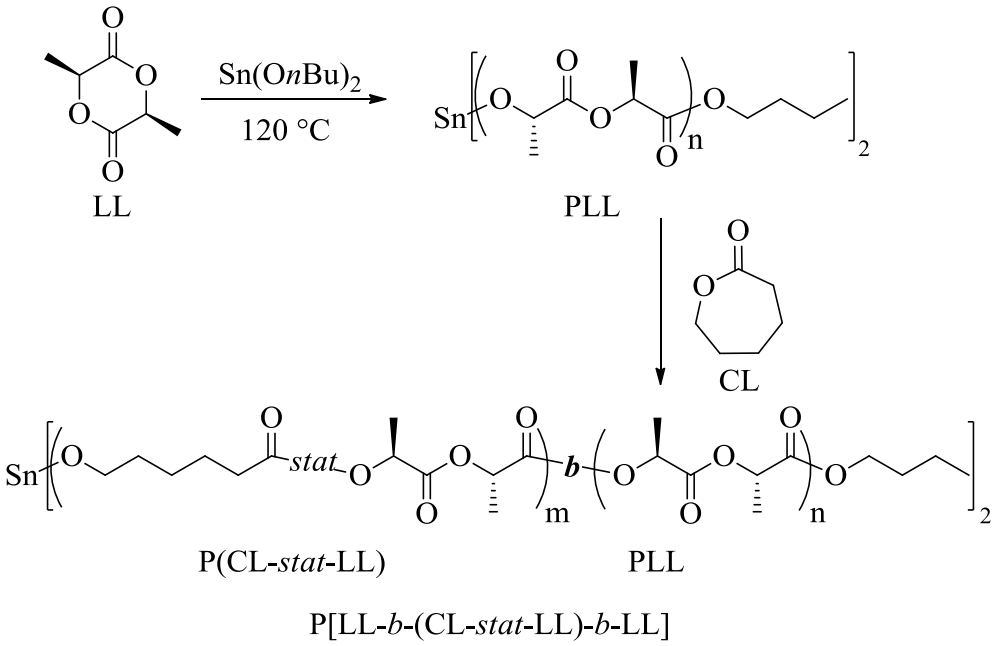

Scheme 2. Two-step copolymerization for P[LL-*b*-(CL-*stat*-LL)-*b*-LL] block copolymers

2.2.1 Nuclear magnetic resonance (NMR) spectroscopy

A Bruker Avance NMR Spectrometer using a high-resolution dual (^{1}H, ^{13}C) gradients probe was employed for structural characterization using deuterated chloroform ($CDCl_3$) and

tetramethylsilane (TMS) as solvent and internal standard. The field frequencies were 300 MHz for ^{1}H-NMR and 75 MHz for ^{13}C-NMR.

2.2.2 Gel permeation chromatography (GPC)

Average molecular weights and dispersities (*Đ*) of all polymers were measured using an Agilent 1100 Series GPC Chromatograph employing mixed-bed gel columns, degassed THF eluent system with 2 % v/v of triethylamine (TEA) and a small amount of toluene as a flow-rate marker at a flow-rate of 1 ml min^{-1} at 40 °C, and a refractive index detector. Narrow molecular weight distribution polystyrene standards were used as column calibration standards.

2.2.3 Differential scanning calorimetry (DSC)

A Mettler Toledo DSC 1 Module with STARe system was employed for characterization of thermal transition temperatures. Samples with a mass of 4-5 mg were encapsulated in an aluminum pan and scanned from -50 to 200 °C at a heating rate of 10 °C min^{-1}. After the sample was held at 200 °C for 1 min, it was cooled down to -50 °C at a cooling rate of 10 °C min^{-1} and then a second heating run performed at 10 °C min^{-1}.

2.2.4 Thermogravimetric analysis (TGA)

Thermogravimetric analysis (TGA) of the synthesized polymers was carried out using a Perkin-Elmer TGA7 Thermogravimetric Analyzer. Each polymer sample (5-10 mg) was heated over the temperature range of 50 to 600 °C at a heating rate of 20 °C min^{-1} under a nitrogen atmosphere.

2.2.5 Tensile testing

Homopolymer and copolymer films were prepared by casting from a 10% w/v solution in chloroform to a thickness of approximately 75 μm. Rectangular-shaped specimens of dimensions 7 cm × 1 cm were cut for tensile testing using a Hounsfield HTi Tensometer with a 50 N load cell in accordance with the ASTM D882-02 test method for thin plastic sheeting.[35] Stress-elongation data were recorded at a crosshead speed of 25 mm min^{-1}. At least five specimens were tested for each sample (gauge length 5 cm) at room temperature.

3. Results and Discussion

In this paper, sample codes are used to identify each sample. For example, S(LL62/CL38) is used as the code for a P(LL-*stat*-CL) statistical copolymer prepared from an initial monomer molar ratio of LL:CL = 62:38. Similarly, a P[LL-*b*-(CL-*stat*-LL)-*b*-LL] block copolymer made from a LL:CL ratio of 60:40 is labelled as B(LL60/CL40). The sequence of the LL and CL symbols represents the order in which the monomers were added in the first and second steps. The labels con0.25 and con0.69 indicate how far the fraction of conversion had reached in the first step before the second monomer was added in the second step.

The formation of PCL and PLL prepolymers was verified by ^{1}H-NMR through the appearance of the proton peaks and also the change in chemical shift of protons adjacent to the Sn-O bonds of the initiator, as labelled in Figure 1. The appearance of these latter peaks in the prepolymer spectra is important evidence of the insertion of the monomer into the Sn-O bonds of the $Sn(OnBu)_2$ initiator. The two different (a) and (a′) peaks in the PCL and PLL prepolymers are related to the asymmetry of the polymer chain on either side of the initiator while the broader (a″) peak in $Sn(OnBu)_2$ is due to molecular aggregation.[11]

The LL and CL contents were calculated from the ^{1}H-NMR spectra by integrating the proton peak areas at chemical shifts (δ) of 5.17, 4.08 and 2.33 ppm assigned to CH in LL, ε-CH_2 in CL and α-CH_2 in CL respectively, as shown in Figure 2. The $\overline{M}_n$ values of the prepolymers were estimated by comparing the peak area integration of the polymer proton signal (from the first step polymer) to that of the -O*n*Bu butoxy end-group.[36-37]

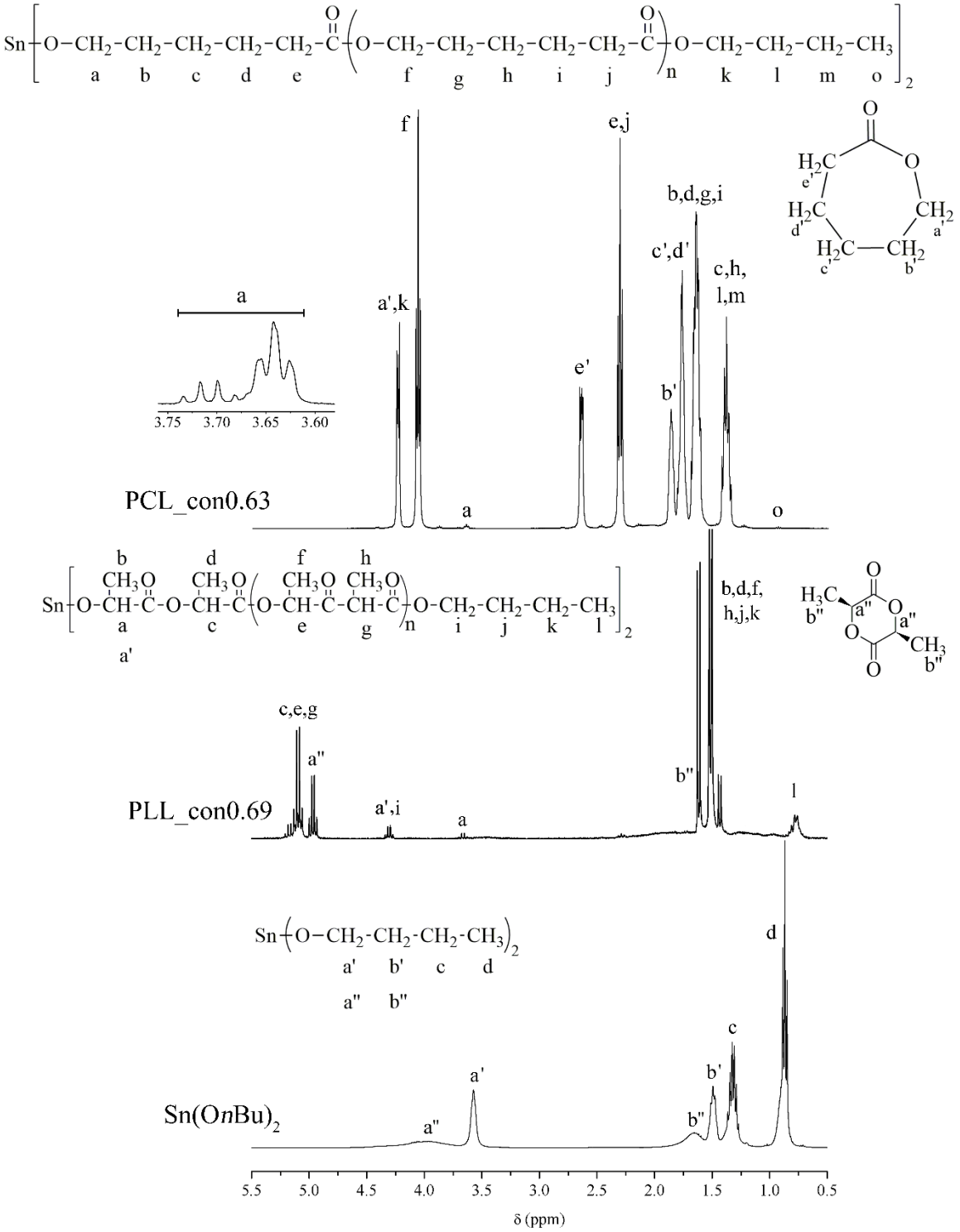

Figure 1. 300 MHz ^{1}H-NMR spectra of PCL_con0.63 (top), PLL_con0.69 (middle) and Sn(O*n*Bu)$_2$ (bottom) in $CDCl_3$

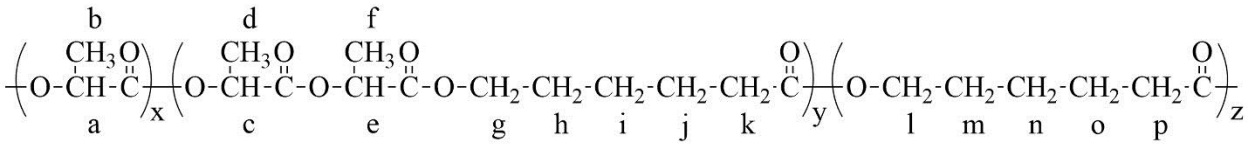

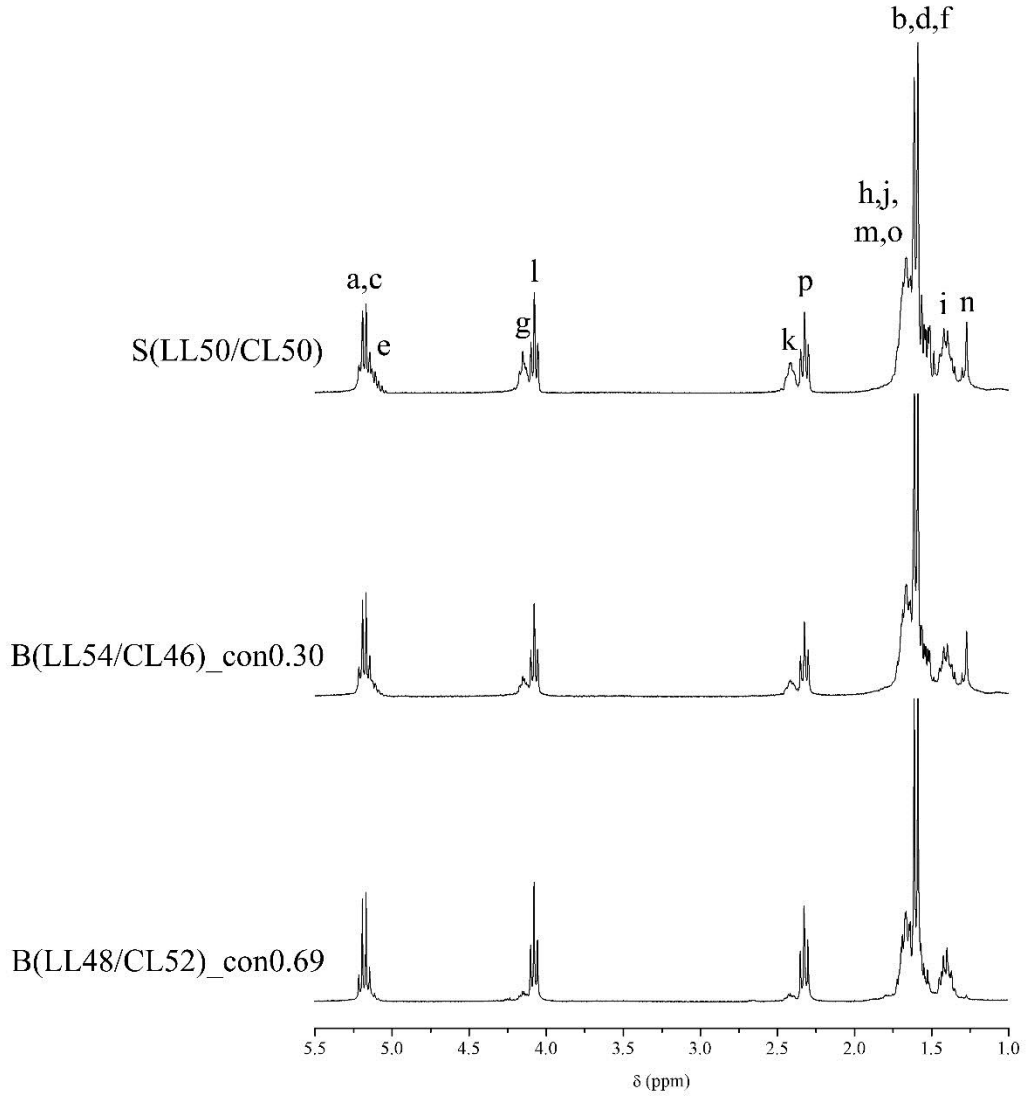

Figure 2. 300 MHz ^{1}H-NMR spectra of S(LL50/CL50) (top), B(LL54/CL46)_con0.30 (middle) and B(LL48/CL52)_con0.69 (bottom) in $CDCl_3$

From ^{13}C-NMR, the average sequence lengths of the lactidyl (l_L) and caproyl (l_C) units as well as the degree of randomness (R) could be calculated by integrating the peak areas of the

carbonyl carbon peaks of the LCC, CCL, LCL, LLC and CLL triad sequences[38-39], as shown in Figure 3.

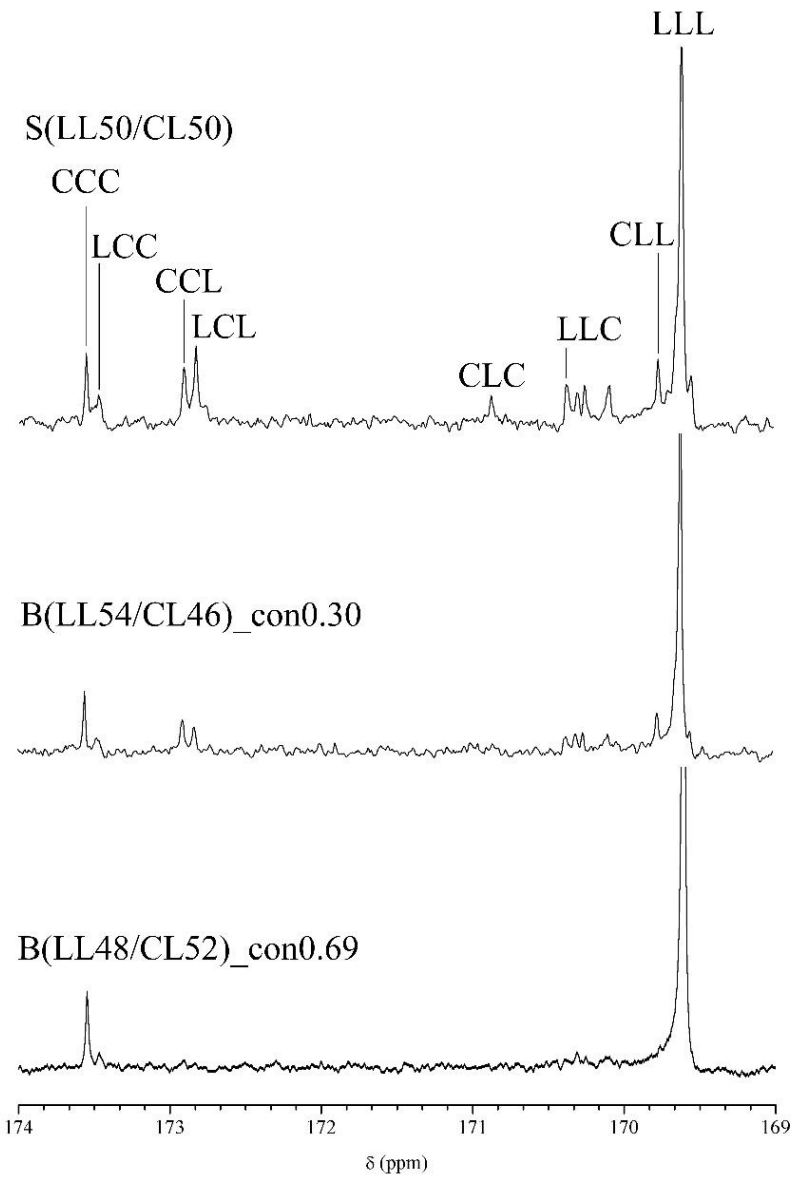

Figure 3. 75 MHz ^{13}C-NMR spectra (expanded carbonyl carbon regions) of S(LL50/CL50) (top), B(LL54/CL46)_con0.30 (middle) and B(LL48/CL52)_con0.69 (bottom) in $CDCl_3$

The equations for calculating l_L and l_C are shown in equations (1) and (2) respectively.[12,17-18]

$$l_L = \frac{1}{2}\left[\frac{I_{LLL} + (I_{LLC} + I_{CLL})/2}{(I_{LLC} + I_{CLL})/2 + I_{CLC}} + 1\right] \quad (1)$$

$$l_C = \frac{I_{CCC} + I_{LCC}}{I_{CCL} + I_{LCL}} + 1 \quad (2)$$

where I is the integral of the various central carbonyl carbon signals attributed to the triad sequences and the subscripts L and C refer to the lactidyl, -O-CH(CH_3)-CO-, and caproyl, -O-(CH_2)$_5$-CO-, repeat units.

The l_L and l_C values for the synthesized copolymer chains can be compared with those for a random distribution of lactidyl (l_L^R) and caproyl (l_C^R) units which can be calculated from equations (3) and (4).[12-14,38]

$$l_L^R = \frac{(k+1)}{2k} \quad (3)$$

$$l_C^R = (k+1) \quad (4)$$

where k is the [C]/[L] molar ratio. The value of the randomness coefficient (R) of the copolymer chains can then be determined from equation (5).[12-14,38]

$$R = \frac{l_L^R}{l_L} = \frac{l_C^R}{l_C} \quad (5)$$

At the microscopic level, the value of R reflects the microstructure of the copolymer chain, ranging from 0 for a diblock to 1 for a completely random copolymer. This then manifests itself at the macroscopic level in terms of how R affects various physical properties. For example, the higher the value of R, the less likely that the copolymer can crystallize which in turn affects its thermal (temperature transitions) and mechanical properties. Thus, the value of R is a useful

indicator of what type of material the copolymer is likely to be in between the two extremes of its parent homopolymers. The various microstructural parameters, monomer conversions (α) and average molecular weights of the prepolymer and final products are summarized in Table 1.

Table 1. Polymerization data of LL and/or CL using 0.10 mol % Sn(O*n*Bu)$_2$ at 120 °C for 12 h

Polymers	α	$\bar{M}_n$ [a)]	f_{LL}	F_{LL} [b)]	l_L [b)]	l_C [b)]	R [b)]	$\bar{M}_n$ [b)]	$\bar{M}_w$ [b)]	$Đ$ [b)]	%Yield[b)]
PLL	-	-	1.00	1.00	-	-	-	1.90×10^5	2.75×10^5	1.45	96.6
PCL	-	-	0.00	0.00	-	-	-	1.30×10^5	1.68×10^5	1.29	95.9
S(LL/CL)	-	-	0.33	0.35	1.10	2.48	0.70	1.49×10^5	1.94×10^5	1.30	94.4
	-	-	0.50	0.50	1.40	2.46	0.72	1.66×10^5	2.12×10^5	1.27	95.7
	-	-	0.60	0.62	1.79	1.53	0.74	2.08×10^5	2.51×10^5	1.21	94.5
	-	-	0.67	0.68	1.93	1.19	0.82	1.89×10^5	2.35×10^5	1.24	95.0
B(LL/CL)	0.32	1.6×10^4	0.33	0.36	2.91	2.86	0.26	9.29×10^4	1.40×10^5	1.51	92.6
	0.30	1.3×10^4	0.50	0.54	3.28	2.41	0.32	1.31×10^5	1.74×10^5	1.33	90.2
	0.25	9.4×10^3	0.60	0.60	3.86	2.14	0.32	9.53×10^4	1.29×10^5	1.35	90.8
	0.21	5.6×10^3	0.67	0.65	4.20	2.00	0.34	1.09×10^5	1.47×10^5	1.34	91.4
	0.69	2.6×10^4	0.50	0.48	6.65	6.14	0.14	1.47×10^5	1.89×10^5	1.28	81.0
B(CL/LL)	0.25	1.3×10^4	0.33	0.40	2.98	3.04	0.28	9.01×10^4	1.11×10^5	1.23	51.7
	0.25	9.4×10^4	0.50	0.59	4.13	2.46	0.30	7.59×10^4	9.70×10^4	1.28	52.7
	0.30	8.8×10^4	0.60	0.63	6.51	2.41	0.20	1.31×10^5	1.75×10^5	1.33	52.2
	0.29	7.1×10^4	0.67	0.71	7.08	2.17	0.24	9.99×10^4	1.14×10^5	1.14	50.1
	0.63	2.3×10^4	0.50	0.57	7.55	7.08	0.12	1.16×10^5	1.50×10^5	1.29	81.1

[a)] For the first-step prepolymer; [b)] for the final second-step copolymer; α = first-step monomer fraction of conversion.

The results in Table 1 show that the molar ratios of LL and CL in the final copolymers closely match the initial monomer feed ratios. The final LL compositions (F_{LL}) in S(LL/CL) and B(LL/CL) were close to the initial LL monomer feed mole fractions (f_{LL}) whereas those in

B(CL/LL) were significantly higher. From GPC, the synthesized polymers showed $\bar{M}_n$ in the range of 7.6×10^4 to 2.8×10^5 with unimodal molecular weight distributions and relatively low dispersities (*Đ*) ranging from 1.14 to 1.51. The percentage yields (% by weight) of PCL, PLL and S(LL/CL) were all over 94% but slightly lower (90-93%) in B(LL/CL) while in B(CL/LL) the percentage yield decreased to about 50% under the same conditions.

These results can be partly explained by the higher monomer reactivity of LL compared to CL.[17,30,40] Lin *et al*.[17] considered the LL and CL monomer reactivities in terms of the negative charge densities on the carbonyl oxygens. Even though the carbonyl group in CL has a higher electron density than that in LL, there are two carbonyl groups in a single molecule of LL which contributes to its higher polymerizability. Thus, the results suggest that longer polymerization times and/or higher polymerization temperatures should be employed in order to increase the lower percentage yield of B(CL/LL). From ^{13}C-NMR, l_L increased with increasing LL content as did the value of l_C with CL content. As expected, the values of l_L and l_C for both B(CL/LL) and B(LL/CL) were higher than those for S(LL/CL), while the latter had higher values of *R*. Thus, it can be confirmed that, as predicted, two-step sequential monomer addition produced blockier structures than single-step copolymerization. Since the reactivity ratio of LL is higher than that of CL, the S(LL/CL) produced is a statistical (rather than a purely random) copolymer[18], as represented in Figure 4 (a). In the two-step procedure, the final products were P[LL-*b*-(CL-*stat*-LL)-*b*-LL] and P[CL-*b*-(LL-*stat*-CL)-*b*-CL] block copolymers consisting of a central statistical copolymer block flanked by two blocks comprising just one monomer, as represented in Figures 4 (b) and (c).

In contrast, previous results showed that, although the active PLL did initiate CL in a sequential copolymerization, the resulting copolymer had more of a random/statistical distribution of monomers than would be expected for a block copolymer microstructure.[20-26] This was

attributed to the occurrence of transesterification reactions caused by the CL-derived hydroxyl end-groups generated during the second-step copolymerization, as also observed by other workers.[20-26,30]

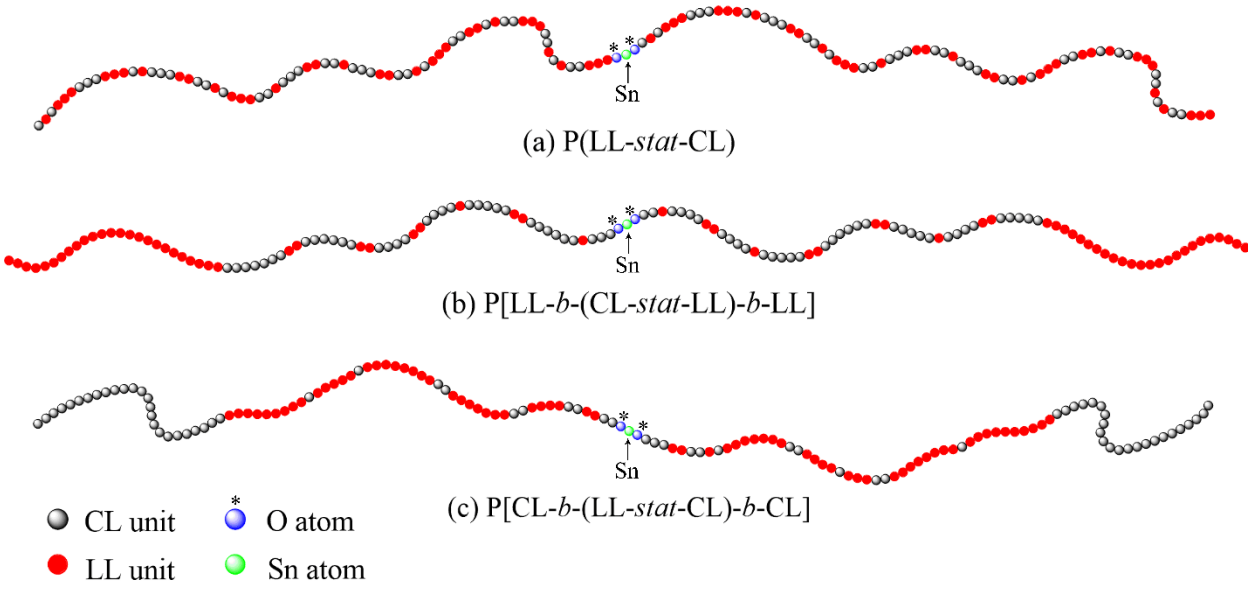

Figure 4. Chain microstructure representations of P(LL-*stat*-CL) (a), P[LL-*b*-(CL-*stat*-LL)-*b*-LL] (b) and P[CL-*b*-(LL-*stat*-CL)-*b*-CL] (c) copolymers each with equimolar LL(●):CL(●) 50:50 compositions

In other work, Florczak *et al.*[30] compared the efficiencies in synthesizing B(LL/CL) of different initiating systems such as tin(II) octoate [$Sn(Oct)_2$] in butanol (BuOH), aluminum tris-isopropoxide [$Al(O^iPr)_3$] and $Al(O^iPr)_3$ in (*S*)-(+)-2,2′-[1,1′-binaphtyl-2,2′-diylbis(nitrylomethilidyne)]diphenolate [$SB(OH)_2$] as a bulky ligand. They reported that only the $Al(O^iPr)_3/SB(OH)_2$ initiating system could produce a block copolymer of B(LL/CL) due to the steric hindrance of the bulky $SB(OH)_2$ ligand reducing the tendency for transesterification. In comparison, the results here have shown that, although $Sn(OnBu)_2$ is not a bulky initiator, the B(LL/CL) block copolymer can be obtained if the polymerization time is kept relatively short since

transesterification can occur with prolonged reaction times under monomer-starved conditions.[38] Block copolymers at higher first-step conversion (69%) showed higher values of l_L and l_C as well as lower R values than those at lower first-step conversion (30%), as would be expected. This was because, at the higher first-step conversion, the second monomer could form longer segments within the statistical copolymer block due to its relatively high concentration compared with the lower amount of residual first step monomer.

Thermal analysis of the synthesized polymers and copolymers was carried out using DSC. Examples of the thermograms (2nd heating scans) are shown in Figure 5 and the derived values of T_g, T_c and T_m as well as the heats of crystallinity (ΔH_c) and melting (ΔH_m) are compared in Table 2.

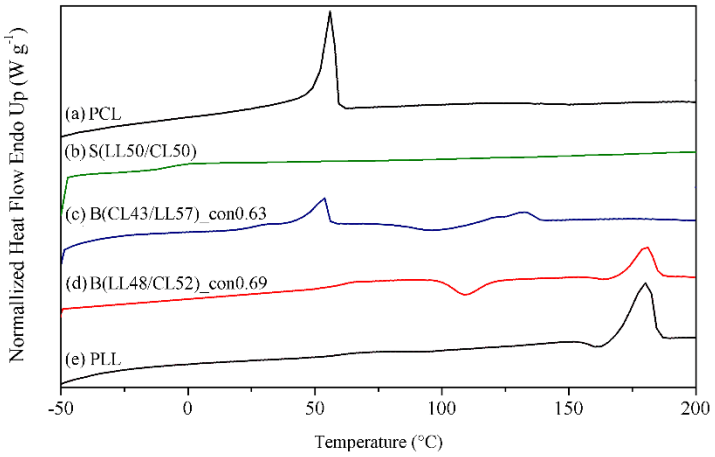

Figure 5. DSC thermograms (2nd heating scans) of (a) PCL, (b) S(LL50/CL50), (c) B(CL43/LL57)_con0.63, (d) B(LL48/CL52)_con0.69 and (e) PLL

Table 2. Temperatures, heats of transition (the second DSC heating scans) of the PLL, PCL and LL/CL copolymers

Polymers/Copolymers	T_g (°C)	$T_m^{a)}$ (°C)	$\Delta H_m^{a)}$ (J g^{-1})	$X_{c,PCL}$ [e)] (%)	T_c (°C)	ΔH_c (J g^{-1})	$T_m^{b)}$ (°C)	$\Delta H_m^{b)}$ (J g^{-1})	$X_{c,PLL}$ [e)] (%)
PLL	63	-	-	-	-	-	181	62	65
PCL	-60[c)]	56	85	60	-	-	-	-	-
S(LL35/CL65)	-23[d)]	-	-	-	-	-	-	-	-
S(LL50/CL50)	-6	-	-	-	-	-	-	-	-
S(LL62/CL38)	32	-	-	-	-	-	152	3	2
S(LL68/CL32)	26	-	-	-	-	-	152	18	19
B(LL36/CL64)_con0.32	-6	43	6	4	-	-	156	9	10
B(LL54/CL46)_con0.30	0	42	2	1	-	-	145	2	1
B(LL60/CL40)_con0.25	-	-	-	-	-	-	156	23	25
B(LL65/CL35)_con0.21	31	-	-	-	-	-	153	31	33
B(LL48/CL52)_con0.69	62	-	-	-	108	31	180	50	53
B(CL60/LL40)_con0.25	-6	55	29	21	-	-	-	-	-
B(CL41/LL59) _con0.25	-	55	20	14	-	-	159	2	2
B(CL37/LL63) _con0.30	51	-	-	-	118	9	156	20	21
B(CL29/LL71) _con0.29	50	-	-	-	97	25	151	25	27
B(CL43/LL57) _con0.63	24	53	27	19	93	12	132	19	20

[a)] PCL melting endotherm at lower temperature; [b)] PLL melting endotherm at higher temperature; [c)] reference T_g value of PCL[41]; [d)] T_g calculated from the Fox equation [$(w_{LL}/T_{gPLL}) + (w_{CL}/T_{gPCL}) = 1/T_{gP(LL\text{-}CL)}$] for comparison, [e]$X_c$ = % crystallility [$(\Delta H_m/\Delta H_m^\circ)\times 00$] where ΔH_m° of PCL[42] and PLA[43] are 139.5 J g^{-1} and 93.1 J g^{-1} respectively.

The S(LL/CL) copolymer created in a one-step copolymerization was amorphous with no melting peak, whereas the two-step B(LL/CL) and B(CL/LL) copolymers were semi-crystalline

with either a PLL melting peak alone or both PLL and PCL melting peaks depending on the sequence of monomer addition. This lends further support for the blockier nature of the copolymers produced by the two-step synthesis in which distinct sequences of like monomer units are required for (homopolymer) crystal formation.[44-45] The results here have shown that crystallizability is mainly governed by the length of the prepolymers blocks formed in the first step reaction.

For a PCL melting peak to appear, the CL monomer must be polymerized first in order to produce sufficiently long PCL block lengths for crystallization to occur. Another notable feature from Table 2 is that a clear PLL T_g and T_c were only observed for the B(LL48/CL52) sample at higher first-step conversion (69%) which is also attributed to longer (in this case PLL) block lengths. Thus, the sequence of monomer addition and the first-step conversion are both influential factors in controlling the semi-crystalline morphology of the block copolymer.

The TGA profiles in Figure 6 demonstrate the higher thermal stability of PCL compared to PLL due to its lower main-chain (backbone) concentration of ester groups. As a result, the block copolymers with longer block lengths tended to exhibit two-step degradation profiles. This was particularly evident in the case of B(LL48/CL52)_con 0.69. The higher the degree of randomness in the copolymer, the higher the thermal stability. This can be attributed to the insertion of CL units into the PLL blocks separating the LL ester groups and thereby lowering the tendency for PLL depolymerization. This results in a higher thermal stability in the more random (i.e., statistical) copolymers than in the block copolymers. Additionally, B(CL/LL) exhibited a lower thermal stability than B(LL/CL) at a similar composition, molecular weight and length of the first block prepolymer due to its blockier microstructure.

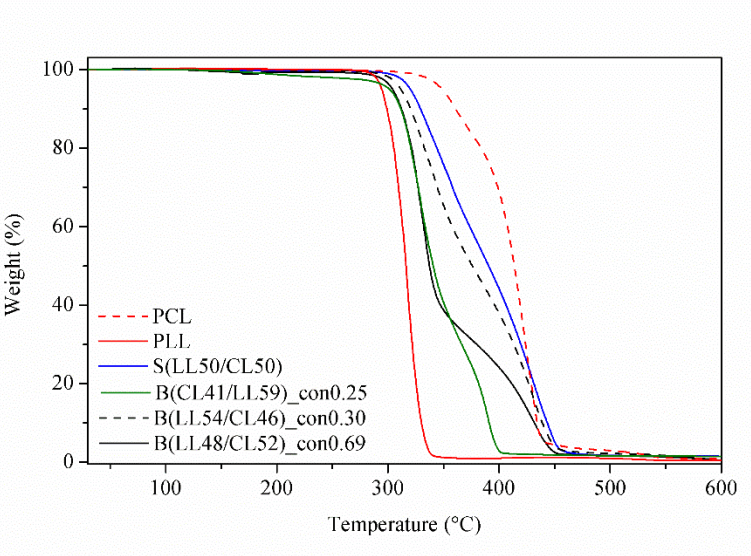

Figure 6. Non-isothermal TG thermograms of PCL, PLL, S(50LL/CL50), B(CL41/LL59)_con0.25, B(LL54/CL46)_con0.30 and B(LL48/CL52)_con0.69

Examples of the stress-strain curves from the tensile testing of thin films of the block copolymers are shown in Figure 7 and the values of stress at break, strain at break and Young's modulus shown in Figure 8. The stress-strain curves showed the characteristics of plastic behaviour, but with considerable variation – reflecting the different microstructures of the individual copolymers. Homopolymers of the constituent monomers showed very different behaviour which reflects the fact that at room temperature PLL is below its T_g, whereas PCL is well above its T_g. PLL was seen to fracture abruptly at low (*ca.* 8%) strain, reflecting a tendency to undergo brittle fracture. The sequence of five methylene groups that seperate the repeating ester groups in PCL dilute the dipolar interchain and intrachain interaction. As a consequence, PCL showed properties of a flexible (ductile) material and a much higher elongation at break. In addition, the thermal analysis data (Table 2) enable the approximate crystallinities of the

homopolymers to be calculated. As expected, the crystallinity of the PLL sample (*ca.* 65%) is higher than that of the PCL sample (*ca.* 60%).

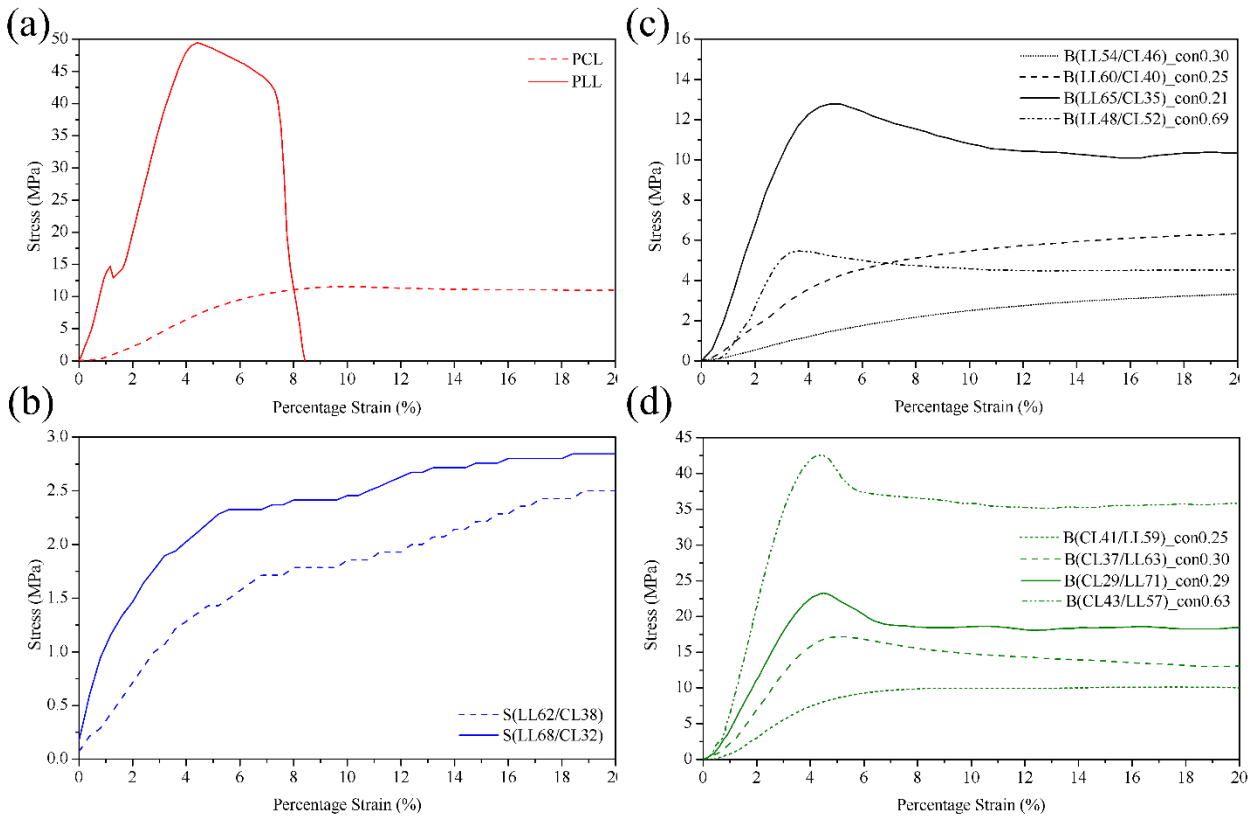

Figure 7. Stress-strain curves of (a) the PCL and PLL homopolymers, (b) S(LL/CL) of different compositions, and (c) B(LL/CL) and (d) B(CL/LL) of different compositions with the CL and LL added at different % conversions

In order to compare the effects of copolymer microstructure, it is necessary to compare the initial slopes from which the Young's moduli are calculated and the characteristics of the "yield point" region. The sequence of structural changes of semi-crystalline polymers during elongation are described in terms of elongation of the amorphous regions and alignment and sliding of the crystalline regions. The factors that affect the polymer microstructure in this family of block

copolymers are (i) the choice of monomer for the first block; (ii) the proportions of monomers used in the copolymer and (iii) the % conversion of the first block at the point of addition of the second monomer. Manipulation of these three input parameters in the polymer chemistry stage allows intimate control of the physical and mechanical properties of the final polymer. In the case of statistical copolymers, both monomers are added together and their relative reactivities and final conversion govern the microstructure. The overall molecular weights of the copolymers (Table 1) are not sufficiently different to produce a tangible effect.

Statistical copolymers will inevitably produce polymers with reduced sequence lengths of the individual monomers and consequent reduction in melting point and % crystallinity. This is normally associated with a detrimental effect on mechanical properties, particularly stiffness, as shown in the data in Figure 8, where the Young's modulus typically increases as the approximate overall % crystallinity (X_c) increases within the same type of copolymer. However, if we take a closer look at the block copolymers, a more interesting pattern emerges. The stiffness of the block copolymers is influenced more by the amount of PCL crystallinity ($X_{c,PCL}$) in the system than the total degree of crystallinity; the higher $X_{c,PCL}$, the higher the Young's modulus. Consequently, the B(CL/LL) polymers (where CL was polymerized first) were generally stiffer than their B(LL/CL) counterparts of equal content, even with the same total X_c. This is attributed to the low T_g of PCL, which is below room temperature, and therefore needs crystalline regions to provide stiffness. In short, when designing polymers, it is important to control not only the total degree of crystallinity, but also the type of crystallized domains within the material.

Of the statistical copolymers shown in Table 2, S(LL35/CL65) and S(LL50/CL50) were too soft to cut acceptable tensile dumbbells whereas the statistical copolymers with higher LL contents gave no such problems. Interestingly, two of the block copolymers were too soft for

tensile studies, but for rather different reasons. The properties of B(LL36/CL64)_con0.32 were impaired by the low overall LL content coupled with the low (32%) conversion of LL to form the first block. This resulted in an extremely low proportion of LL sequences. Although B(CL60/LL40)_con0.25 had a somewhat higher proportion of LL (40%) this was impaired by the fact that the first (CL) block was taken to only 25% conversion before additiion of the LL. Consequently, the second block was essentially a statistical copolymer containing comparable proportions of CL and LL.

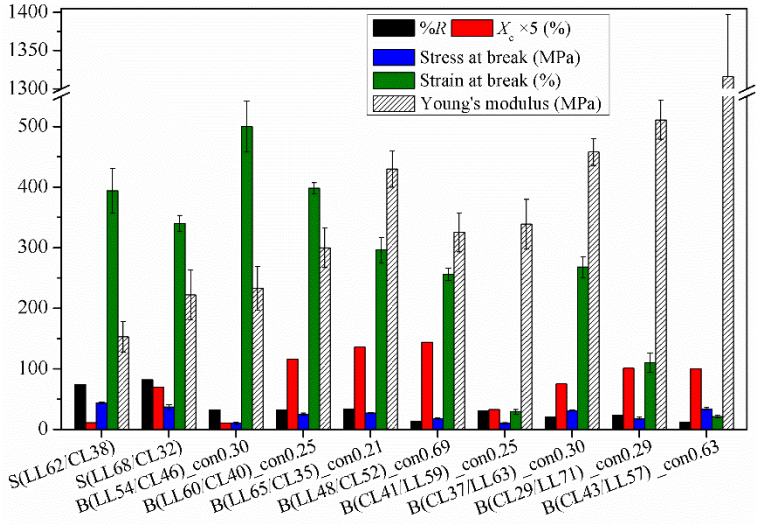

Figure 8. Comparison of the values of %*R*, total X_c, stress at break, strain at break and Young's modulus of PLL, PCL and the various P(LL/CL) copolymers. *Note:* total X_c is the approximate total degree of crystallinity based on $X_c = (X_{c,\,PCL} \times w_{PCL}) + (X_{c,\,PLL} \times w_{PLL})$ from Table 2.

These observations provide a sound basis for interpreting the behaviour of the remaining block copolymers studied here. Thus, the stiffest materials obtained when CL is used as the first monomer are those in which the CL block is taken to high conversion before addition of LL. This principle extends throughout the whole of the group and is related to the fact that lower conversions

of CL mean that there is more CL monomer available to ‘contaminate’ the LL block – essentially converting it into a statistical copolymer block.

It is clear that the stiffest block copolymers are those that contain higher proportions of LL; the copolymers in which LL form the first block at higher proportions tend to show higher yield stress (Figure 7c). This is because a higher amount of ‘uncontaminated’ PLL sequences conveys properties more akin to those of PLL. Thus, within this group, block copolymers are produced in which the modulus is reduced to around 50% compared to PLL homopolymer, but are enhanced with a much higher elongation at break. Similarly, when CL forms the first block and is taken to high conversion [e.g. B(CL43/LL57 con 0.63)], Figure 7d, moduli relatively similar to that of PLL homopolymer can be produced but with an approximately three-fold increase in elongation at break. The key point to note is that the mechanical properties of the copolymers can be manipulated through microstructural control (by monomer content and sequencing and first block conversion, as afore-mentioned). This capability is of particular importance where the tailoring of polymer properties to meet specific requirements is concerned.

One final feature of the stress-strain curves is the gradual increase in the slope beyond the yield point. This is conventionally interpreted as a strain-hardening effect due to the increase in molecular alignment. Interestingly, this phenomenon is very structure-dependent and of all the copolymers studied it is the statistical copolymers with high proportions of LL [e.g. S(LL65/CL35 con 0.21), Figure 8b] that show the most effective strain-hardening capability. This feature, which is beyond the scope of the work described herein, could potentially also be exploited in the control of desired mechanical properties for specific applications.

4. Conclusions

The synthesis of LL/CL copolymers with a wide range of chain microstructures has been achieved using various compositions and two different polymerization procedures. In this work, the average sequence lengths of the lactidyl (l_L) and caproyl (l_C) units synthesized via the two-step procedure were longer than those via the one-step procedure. As a result, single-step copolymerization yielded P(LL-*stat*-CL) statistical copolymers while P[LL-*b*-(CL-*stat*-LL)-*b*-LL] and P[CL-*b*-(LL-*stat*-CL)-*b*-CL] block copolymers were obtained from two-step sequential copolymerization. Moreover, the order of monomer addition affected the block copolymer microstructure with P[LL-*b*-(CL-*stat*-LL)-*b*-LL] having slightly more randomness than P(CL-*b*-[LL-*stat*-CL]-*b*-CL) due to the differing reactivity ratios of the monomers. Adding the second monomer at a higher first step conversion gave blockier copolymers. One-step P(LL-*stat*-CL) copolymers were shown to be amorphous, whereas the two-step P[LL-*b*-(CL-*stat*-LL)-*b*-LL] and P(CL-*b*-[LL-*stat*-CL]-*b*-CL) block copolymers were semi-crystalline.

The thermal and mechanical properties of the copolymers were, in general, intermediate between those of PCL and PLL. Block copolymers tended to reflect the lower thermal stability of PLL. Tensile testing produced stress-strain curves with a range of plastic deformation behaviours. The block copolymers with higher LL contents and/or block lengths exhibited two-step composite curves showing an initial hard-brittle response characteristic of the PLL followed by a soft-ductile response characteristic of PCL. These clearly demonstrated that the toughness and flexibility of LL-CL copolymers can be manipulated by the copolymerization procedure, the sequence of incorporation and the % conversion of the first block. This versatility creates the potential for tailoring copolymer properties to meet specific requirements for individual biomedical applications.

Conflict of Interest

The authers declear that they have no conflict of interest.

Acknowledgements

S.P. wishes to thank the Research Professional Development Project under the Science Achievement Scholarship of Thailand (SAST) for the provision of a PhD scholarship and also the Graduate School, Chiang Mai University. This research work was partially supported by the Center of Excellence in Materials Science and Technology, Chiang Mai University.

References

1 Stridsberg K, Ryner M, Albertsson A-C. Degradable aliphatic polyesters. In: Albertsson A-C (ed). Adv Polym Sci, Vol. 157, Berlin: Springer, 2002; 41-65.

2 Duda A, Kowalski A, Penczek S, Uyama H, Kobayashi S, *Macromolecules* **35 (11):** 4266-4270 (2002).

3 Albertsson AC, Varma IK. Degradable aliphatic polyesters. In: Albertsson A-C (ed). Adv Polym Sci, Vol. 157, Berlin: Springer, 2002; pp 1-40.

4 Vert M, Schwach G, Engel R, Coudane J, *J Control Release* **53:** 85-92 (1998).

5 Seyednejad H, Ghassemi AH, van Nostrum CF, Vermonden T, Hennink WE, *J Control Release* **152 (1):** 168-176 (2011).

6 Pounder R J, Dove AP, *Polym Chem* **1:** 260-271 (2010).

7 Albertsson A-C, Varma IK, *Biomacromolecules* **4:** 1466-1486 (2003).

8 Vaz CM, van Tuijl S, Bouten CVC, Baaijens FPT, *Acta Biomater* **1:** 575-582 (2005).

9 Löfgren A, Albertsson A-C, Dubois P, Jérôme R, *J Macromol Sci C* **35:** 379-418 (1995).

10 Mecerreyes D, Jérôme R, Dubois P. Novel macromolecular architectures based on aliphatic polyesters: Relevance of the "coordination-insertion" ring-opening polymerization. In: Hilborn

JG, Dubois P, Hawker CJ, Hedrick JL, Hilborn JG, Jérôme R, Kiefer J, Labadie JW, Mecerreyes D, Volksen W (eds). Macromolecular Architectures, Vol. 147, Berlin: Springer, 1999; 1-59.

11 Kowalski A, Libiszowski J, Duda A, Penczek S, *Macromolecules* **33 (6):** 1964-1971 (2000).

12 Nalampang K, Molloy R, Punyodom W, *Polym Adv Technol* **18:** 240-248 (2007).

13 Wei Z, Liu L, Yu F, Wang P, Qu C, Qi M, *Polym Bull* **61:** 407-413 (2008).

14 Wei Z, Liu L, Qu C, Qi M, *Polymer*. **50:** 1423-1429 (2009).

15 Qian HT, Bei JZ, Wang SG, *Polym Degrad Stab* **68:** 423-429 (2000).

16 Contreras J, Davila D, *Polym Int* **55:** 1049-1056 (2006).

17 Lin L, Xu Y, Wang S, Xiao M, Meng Y, *Eur Polym J* **74:** 109-119 (2016).

18 Fernández J, Etxeberria A, Sarasua J-R, *J Mech Behav Biomed Mater* **9:** 100-112 (2012).

19 Grijpma DW, Pennings AJ, *Polym Bull* **25:** 335-341 (1991).

20 In't Veld PJA, Velner EM, Van De Witte P, Hamhuis J, Dijkstra PJ, Feijen J, *J Polym Sci A Polym Chem* **35:** 219-226 (1997).

21 Pensec S, Leroy M, Akkouche H, Spasshy N, *Polym Bull* **45:** 373-380 (2000).

22 Zhang L, Shen Z, Yu C, Fan L, *J Polym Sci A Polym Chem* **41:** 927-935 (2004).

23 Stassin F, Jerome R, *J Polym Sci A Polym Chem* **43:** 2777-2789 (2005).

24 Chmura AJ, Davidson MG, Jones MD, Lunn MD, Mahon MF, Johnson AF, Khunkamchoo P, Roberts SL, Wong SSF, *Macromolecules* **39:** 7250-7257 (2006).

25 Keram M, Ma H, *Appl Organometal Chem* **31:** e389 (2017).

26 Slattery RM, Stahl AE, Brereton KR, Rheingold AL, Green DB, Fritsch JM, *J Polym Sci A* **57 (1):** 48-59 (2018).

27 Zhong X, Yu D, Meng F, Gan Z, Jing X, *Polym J* **31:** 633-636 (1999).

28 Kalmi M, Lahcini M, Castro P, Lehtonen O, Belfkira A, Leskela M, Repo T, *J Polym Sci A Polym Chem* **42 (8):** 1901-1911 (2004) .

29 Amgoune A, Thomas ChM, Roisnel T, Carpentier J-F, *Chem Eur J* **12:** 169-179 (2006).

30 Florczak M, Libiszowski J, Mosnacek J, Duda A, Penczek S, *Macromol Rapid Comm* **28:** 1385-1391 (2007).

31 Teng C, Yang K, Ji P, Yu M, *J Polym Sci A Polym Chem* **42:** 5045-5053 (2004).

32 Stevels WM, Ankoné MJK, Dijkstra PJ, Feijen J, *Macromol Chem Phys* **196:** 1153-1161 (1995).

33 Gsell R and Zeldin M, *J Inorg Nucl Chem* **37:** 1133-1137 (1975).

34 Storey RF, Mullen BD, Desai GS, Sherman JW, Tang CN, *J Polym Sci A Polym Chem* **40:** 3434-3442 (2002).

35 ASTM D882-02, Standard test method for tensile properties of thin plastic sheeting, ASTM International, West Conshohocken, *USA* (2002).

36 Gadzinowski M and Sosnowski S, *J Polym Sci A Polym Chem* **41:** 3750-3760 (2003).

37 Pretula J, Slomkowski S, Penczek S, *Adv Drug Deliv Rev* **107:** 3-16 (2016).

38 Kricheldorf HR and Kreiser I, *J Macromol Sci Chem* **24:** 1345-1356 (1987).

39 Kasperczyk J and Bero M, *Angew Makromol Chem* **194:** 913-925 (1993).

40 Piotrowska U, Sobczak M, Oledzka E, *Molecules* **22 (6):** 923-933 (2017).

41 Ferrin DE and English JP. Handbook of biodegradable polymers in *Synthetic absorbable polymers*, ed by Domb AJ, Kost J and Wiseman M. Harwood Academic Publishers, Amsterdam, pp 62-76 (1997).

42 Pitt CG, Chasalow FI, Hibionada YM, *J Appl Polym Sci* **26:** 3779-3787 (1981).

43 Davachi SM and Kaffashi S, *Int J Polym Biomater* **64:** 497-506 (2015).

44 Fernández J, Etxeberria A, Ugartemendia JM, Petisco S, *J Mech Behav Biomed Mater* **12:** 29-38 (2012).

45 Sarasua J-R, Prud'homme RE, Wisniewski M, Borgne AL, Spasshy N, *Macromolecules* **31:** 3895-3905 (1998).

Table of contents

This article describes how the chain microstructure and hence the properties of L-lactide/ε-caprolactone (LL/CL) copolymers can be manipulated through the synthetic procedure. Both one-step and two-step procedures are described leading to statistical and block copolymers respectively. The potential for tailoring the monomer sequencing to meet specific copolymer property requirements is demonstrated.

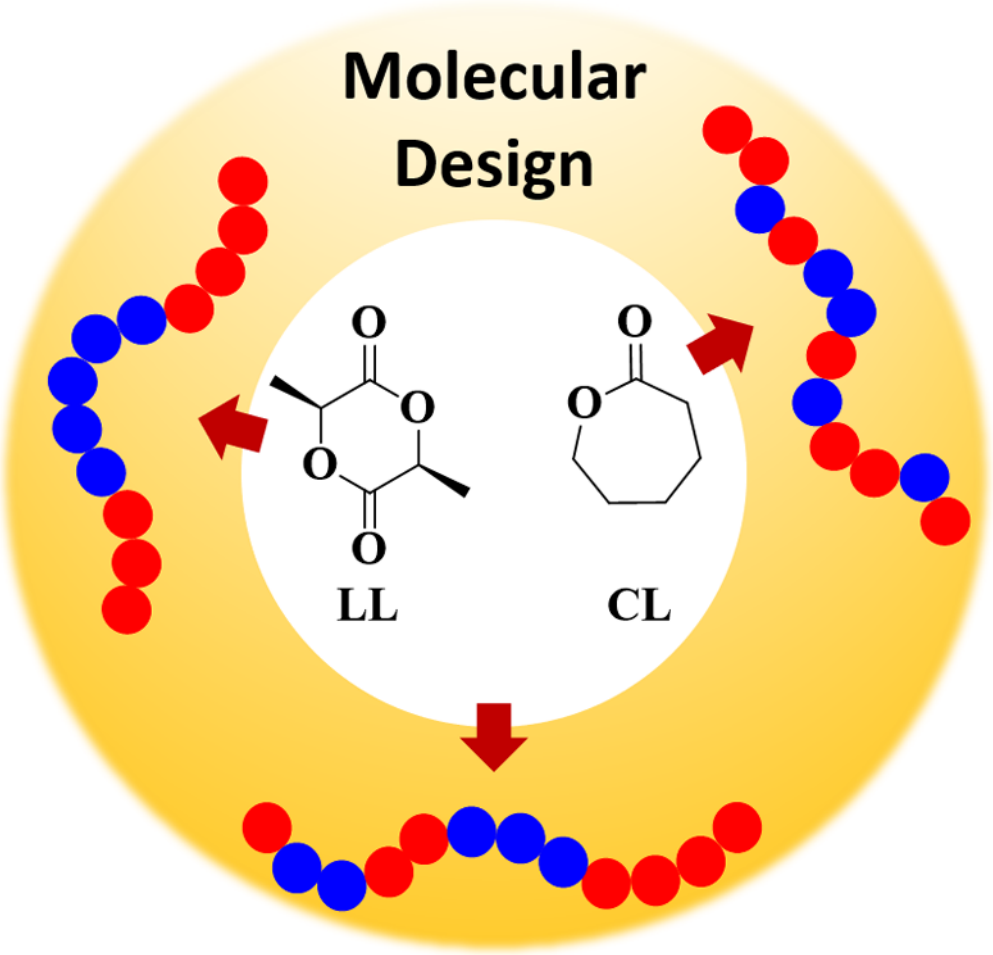
Molecular
Design
O
O
O
O
LL
O
O
CL